Sirolimus attenuates disease progression in an orthologous mouse model of human autosomal dominant polycystic kidney disease

Iram Zafar[1], Kameswaran Ravichandran[1], Franck A. Belibi[1], R. Brian Doctor[2] and Charles L. Edelstein[1]

[1]*Division of Renal Diseases and Hypertension, University of Colorado, Aurora, Colorado, USA and* [2]*Division of Gastroenterology and Hepatology, University of Colorado, Aurora, Colorado, USA*

In autosomal dominant polycystic kidney disease (ADPKD), abnormal proliferation of tubular cells drives cyst development and growth. Sirolimus, an inhibitor of the protein kinase mammalian target of rapamycin (mTOR) and a potent anti-proliferative agent, decreases cyst growth in several genetically distinct rodent models of polycystic kidney disease (PKD). We determined here the effect of sirolimus on renal cyst growth in Pkd2WS25/− mice; an ortholog of human ADPKD involving mutation of the *Pkd2* gene. In Pkd2WS25/− mice treated with sirolimus, both the two kidney/total body weight (2K/TBW) ratio and the cyst volume density (CVD) were significantly decreased by over half compared with untreated mice suffering with PKD. However, there was no effect on the increased blood urea nitrogen (BUN) levels as an index of kidney function. There are two distinct complexes containing mTOR depending on its binding partners: mTORC1 and mTORC2. Western blot analysis of whole kidney lysates and immunohistochemistry of the cysts found that phospho-S6 ribosomal protein, a marker of mTORC1 activity, was increased in Pkd2WS25/− mice and its phosphorylation was decreased by sirolimus treatment. Phospho-Akt at serine 473, a marker associated with mTORC2 activity, was not different between Pkd2WS25/− mice and normal littermate controls. Hence, our study found that inhibition of mTORC1 by sirolimus correlated with decreased renal cyst growth in this model of human ADPKD but had no effect on the decline in renal function.

Kidney International (2010) **78,** 754–761; doi:10.1038/ki.2010.250; published online 4 August 2010

KEYWORDS: polycystic kidney disease; signaling; sirolimus polycystic kidney mouse

Correspondence: *Charles L. Edelstein, Division of Renal Diseases and Hypertension, University of Colorado at Denver and the Health Sciences Center, Box C281, 12700 East, 19th Ave, Aurora, CO 80262, USA. E-mail: Charles.edelstein@ucdenver.edu*

Received 8 January 2010; revised 9 April 2010; accepted 11 May 2010; published online 4 August 2010

We have previously shown in the Han:SPRD rat model of polycystic kidney disease (PKD) that sirolimus treatment decreases proliferation in cystic and non-cystic tubules, markedly inhibits renal enlargement and cystogenesis and prevents the loss of kidney function.[1] Subsequently two other studies have shown that mammalian target of rapamycin (mTOR) inhibition with sirolimus[2] or everolimus[3] reduces cyst formation and renal failure in the Han:SPRD rat. It has also recently been shown that sirolimus decreases cyst formation and renal failure in the orpk-rescue mouse (defective cilia protein polaris) and the bpk mouse (over-expressing myelin and lymphocyte protein) models of PKD.[4] Autosomal dominant polycystic kidney disease (ADPKD) in humans is caused by a mutation in the *Pkd1* or *Pkd2* gene. The Han:SPRD rat, orpk, and bpk mouse do not have primary abnormalities of the *Pkd1* or *Pkd2* genes as the cause of the PKD. In this study, we tested the hypothesis that sirolimus therapy would decrease PKD caused by a mutation in the *Pkd2* gene, in the Pkd2WS25/− mouse model. These mice were engineered to have one of the *Pkd2* alleles knocked out and the other *Pkd2* allele capable of undergoing high rates of recombination with one of the recombination products resulting in the loss of a functional gene. This study in Pkd2WS25/− mice is important as not all therapies that ameliorate murine cystic disease in diverse models may be effective in disease caused by *Pkd* gene mutations and the Pkd2WS25/− mice model closely resembles human ADPKD.

The mTOR exists in association with two different complexes, mTOR complex 1 (mTORC1) and mTOR complex 2 (mTORC2). The mTORC1 is a complex of mTOR and Raptor (regulatory associated protein of mTOR) whereas mTORC2 is a complex of mTOR and Rictor (sirolimus-independent companion of mTOR). The mTORC1 complex regulates cell growth (size), proliferation, apoptosis, and autophagy. Activation of mTORC1 has been shown in PKD in rodents[3–5] and in humans.[6] The effect of PKD and sirolimus on mTORC2 is not known. The mTORC2 increases proliferation, inhibits apoptosis, regulates the actin cytoskeleton, and can phosphorylate Akt at serine 473.[7] As proliferation and apoptosis[8,9] cytoskeleton abnormalities[10,11]

and activation of Akt[3] are features of PKD, the degree of mTORC2 activation was determined.

In this study, we tested the hypotheses that there would be increased mTORC1 and mTORC2 activation in Pkd2WS25/− mouse kidneys and that the mTORC1 inhibitor, sirolimus would decrease PKD in Pkd2WS25/− mice.

RESULTS

Effect of sirolimus on body weight, kidney weight, 2K/TBW, CVD, and BUN

Sirolimus had no effect on the body weight (Table 1). This is in contrast to previous reports showing that short-term (5 week) 0.2 mg/kg/d sirolimus treatment in Han:SPRD rats and wild-type male rats resulted in a 22% loss of body weight.[1] In this study, mice received a higher dose of sirolimus (that is, 0.5 mg/kg/d) for a longer period of time (that is, 8–12 weeks) but did not have weight loss.

Representative kidney sections of vehicle-treated Pkd2WS25/− mice and sirolimus-treated Pkd2WS25/− mice, stained with hematoxylin-eosin, at the same magnification are shown in Figure 1a and b. These representative sections show that the percentage of the kidney that is occupied by cysts is markedly reduced in the kidney obtained from the sirolimus-treated Pkd2WS25/− mice.

The two kidney/total body weight ratio (2K/TBW), which corrects for differences in body weight, was nearly double in Pkd2WS25/− mice compared with vehicle-treated +/+ mice. Sirolimus resulted in a 61% decrease in 2K/TBW (Table 1).

The increase in kidney weights in the Pkd2WS25/− mice was directly paralleled by increases in the measured cyst volume density (CVD) in the kidneys. Mean CVD percentage was 39% in Pkd2WS25/− mice treated with vehicle and 20% in Pkd2WS25/− mice treated with sirolimus. Sirolimus resulted in a 51% decrease in CVD (Table 1).

The blood urea nitrogen (BUN) level was increased in vehicle-treated Pkd2WS25/− mice and sirolimus-treated Pkd2WS25/− mice compared with vehicle-treated +/+ mice and sirolimus-treated +/+ mice. BUN concentration was not different between vehicle-treated Pkd2WS25/− mice and sirolimus-treated Pkd2WS25/− mice (Table 1).

Female Pkd2WS25/− mice have less severe PKD than that that in males.[12] Only two of the ten Pkd2WS25/− vehicle and two of the ten Pkd2WS25/−sirolimus-treated mice were female. The two female Pkd2WS25/− mice treated with sirolimus had a decrease in 2K/TBW (%) and CVD compared with female littermate controls.

In the Pkd2WS25/− model, liver cyst formation increases significantly after 16 weeks of age.[12] This study ended at 16 weeks of age. At the end of the study, liver weight was identical (1.6 g) in Pkd2Ws25/− treated with vehicle and Pkd2Ws25/− treated with sirolimus.

Renal fibrosis

To evaluate renal fibrosis, quantitation of collagen deposition by Masson's trichrome staining was carried out. As shown in Figure 2, sirolimus reduced collagen staining. The renal failure in PKD has been linked to fibrosis. However, despite the reduction in collagen staining by sirolimus, there was no effect on kidney function by sirolimus.

Apotosis and caspase-3

The number of terminal deoxynucleotidyltransferase (TdT)-mediated dUTP nick-end labeling (TUNEL)-positive apoptotic cells per cyst was 0.15 ± 0.06 in Pkd2WS25/− mice treated with the vehicle and 0.26 ± 0.09 in Pkd2WS25/− mice treated with sirolimus (P = not significant vs vehicle-treated, $N = 4$) (Figure 3). Representative pictures of TUNEL staining are shown in Figure 3.

Caspase-3 is the major mediator of apoptosis. In support of the data that there is no significant difference in apoptosis with sirolimus treatment, caspase-3 activity was not

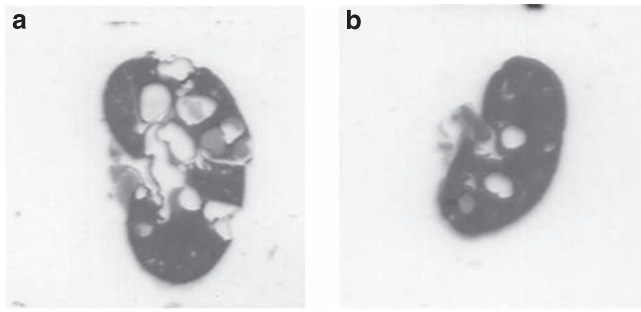

Figure 1 | Effects of sirolimus on polycystic kidney disease (PKD) in Pkd2WS25/− mice. Representative sections at the same magnification, stained with hematoxylin and eosin, show more renal cysts in (**a**) vehicle-treated compared with (**b**) sirolimus-treated Pkd2WS25/− mice.

Table 1 | Effects of sirolimus in Pkd2WS25/− mice

	+/+ vehicle (n=24)	+/+ sirolimus (n=8)	Pkd2WS25/− vehicle (N=10)	Pkd2WS25/− sirolimus (N=10)
Body weight (g)	22.8 ± 3.1	23.4 ± 0.7	27.4 ± 1	27.6 ± 1
Kidney weight (g)	0.31 ± 0.01	0.27 ± 0.02	0.60 ± 0.11*	0.44 ± 0.04**
2K/TBW (%)	1.24 ± 0.02	1.15 ± 0.05	2.20 ± 0.4*	1.63 ± 0.1**
CVD (%)	0.5 ± 0.2	0.5 ± 0.2	38.8 ± 3.7†	20.4 ± 5.1††
BUN (mg/dl)	16.7 ± 0.9	17.5 ± 0.9	33.8 ± 4.2*	29.2 ± 1.5‡

Abbreviations: BUN, blood urea nitrogen; CVD, cystic volume density; NS, not significant; 2K/TBW, two kidney/total body weight.
*P<0.01 vs +/+ vehicle and +/+ sirolimus, **P<0.05 vs Pkd2WS25/− vehicle, NS vs +/+ vehicle and +/+ sirolimus. $^{\dagger}P$<0.001 +/+ vehicle and +/+ sirolimus, $^{\dagger\dagger}P$<0.01 vs Pkd2WS25/− vehicle, ‡NS vs Pkd2WS25/− vehicle. The P-value for the interaction between sirolimus and genotype was NS for kidney weight, NS for 2K/TBW (%), 0.009 for CVD (%) and NS for BUN.

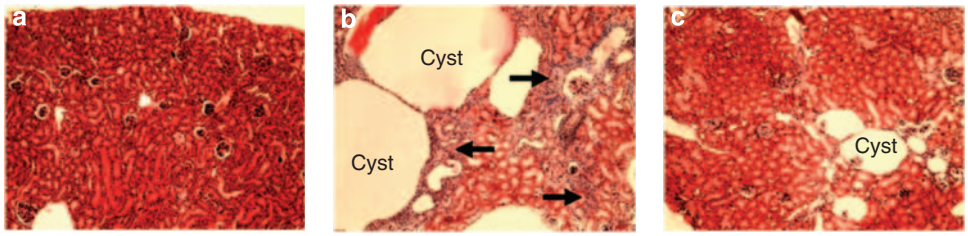

Figure 2 | Representative Masson's Trichrome staining. There was no collagen staining (blue) in control mice (+/+) (**a**). There was extensive collagen staining (blue) (arrows) in Pkd2WS25/− mice (**b**) that was decreased by sirolimus (**c**).

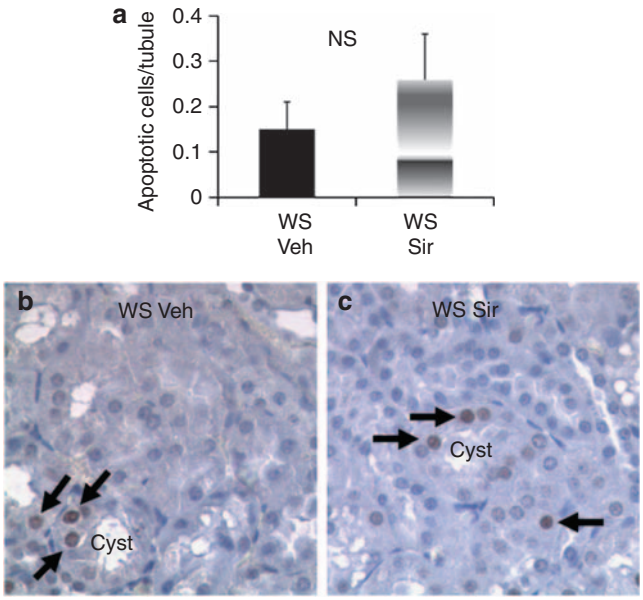

Figure 3 | Representative TUNEL-staining. (**a**) Quantitation of apoptotic cells per tubule. TUNEL-positive tubular cells (dark brown staining, arrows) are shown in Pkd2WS25/− mice treated with vehicle (Veh) (**b**) and Pkd2WS25/− mice treated with sirolimus (Sir) (**c**).

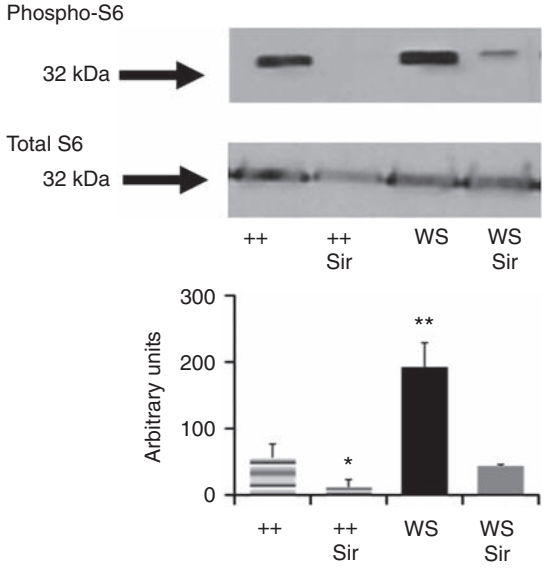

Figure 4 | Phospho-S6 immunoblotting. There was an increase in phospho-S6 protein in cystic and noncystic tubules between normal littermate control (+/+) and Pkd2WS25/− (WS) mice. The increase in phospho-S6 was significantly decreased by sirolimus in normal littermate control (+/+ Sir) and Pkd2WS25/− (WS + Sir). Total S6 used as a control was not different between the groups. Densitometry for phospho-S6 reflects five separate experiments. *$P<0.05$ vs ++, **$P<0.05$ vs ++, **$P<0.05$ vs WS + Sir.

significantly affected by sirolimus. Caspase-3 activity (nmol/min/mg) was 5.4 ± 2.3 in Pkd2WS25/− mice treated with the vehicle and 2.9 ± 1.7 in Pkd2WS25/− mice treated with sirolimus (P = not significant vs vehicle-treated, $N = 5$).

mTORC1 activity

Activation of mTORC1, but not mTORC2, results in the phosphorylation of S6 ribosomal protein. On immunoblotting there was an increase in phospho-S6 ribosomal protein in vehicle-treated Pkd2WS25/− mouse kidneys compared with kidneys from normal littermate controls (+/+) (Figure 4). The increase in phospho-S6 ribosomal protein in Pkd2WS25/− kidneys was inhibited by sirolimus (Figure 4). Total S6 ribosomal protein, used as a control, was not significantly different in vehicle-treated controls (+/+), vehicle-treated Pkd2WS25/−, vehicle-treated Pkd2WS25/−, and sirolimus-treated Pkd2WS25/− kidneys (Figure 4).

To identify the localization of phospho-S6 ribosomal protein, immunohistochemical staining was performed. On immunohistochemical staining, there was increased phospho-S6 ribosomal protein in both noncystic and cystic tubules of Pkd2WS25/− mice. The increase in phospho-S6 ribosomal protein was decreased by sirolimus. Representative pictures of phospho-S6 ribosomal protein staining are shown in Figure 5.

mTORC2 activity

On immunoblotting of whole kidney lysates, Rictor protein was not significantly different between normal littermate controls (+/+) and Pkd2WS25/− mice kidneys (Figure 6a). Interestingly, sirolimus treatment of Pkd2WS25/− resulted in a significant decrease in the abundance of Rictor (Figure 6b).

Phospho-AKT (serine 473) is directly phosphorylated by mTORC2 and phospho-AKT is a marker of mTORC2 activation.[13–15] Phospho-AKT (serine 473) was not different in whole kidney lysates between normal littermate controls and Pkd2WS25/− kidneys (Figure 7a). Furthermore,

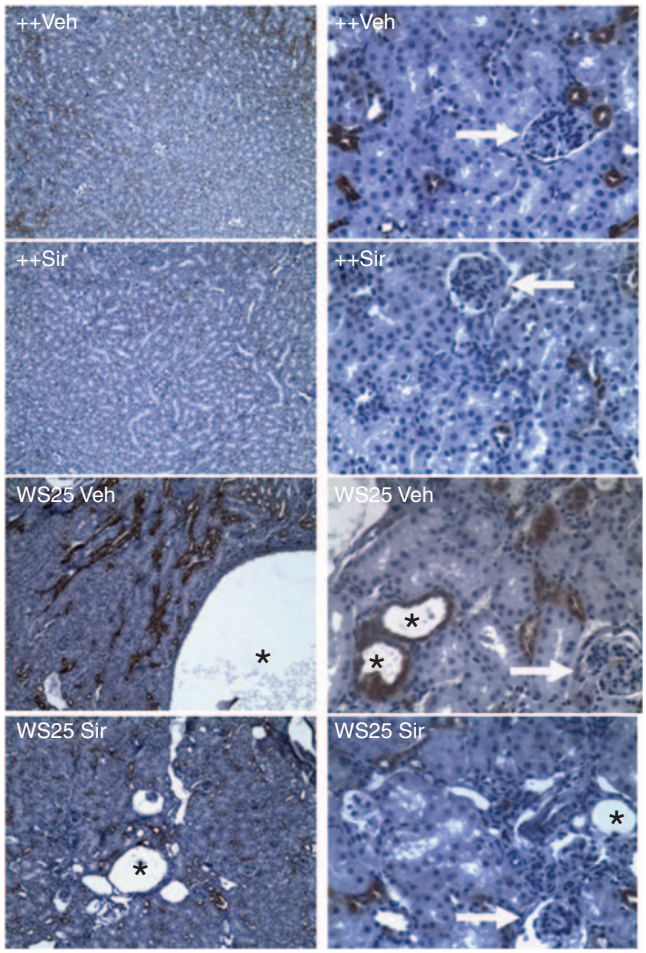

Figure 5 | Phospho-S6 immunohistochemistry. Left panel 100 × magnification. Right panel 400 × magnification. Phospho-S6 staining is brown. There was less staining in sirolimus-treated normal littermate controls compared with vehicle-treated normal littermate controls. There was less staining in Pkd2DWS25/− sirolimus-treated compared with Pkd2WS25/− vehicle treated. There was staining in normal tubules in vehicle-treated normal littermate controls and to a lesser extent in sirolimus-treated normal littermate controls. There was staining in noncystic tubules and small cysts in Pkd2WS25/− vehicle treated and to a lesser extent in Pkd2WS25/− sirolimus-treated. There was no staining in glomeruli (arrows). Asterisk = cysts.

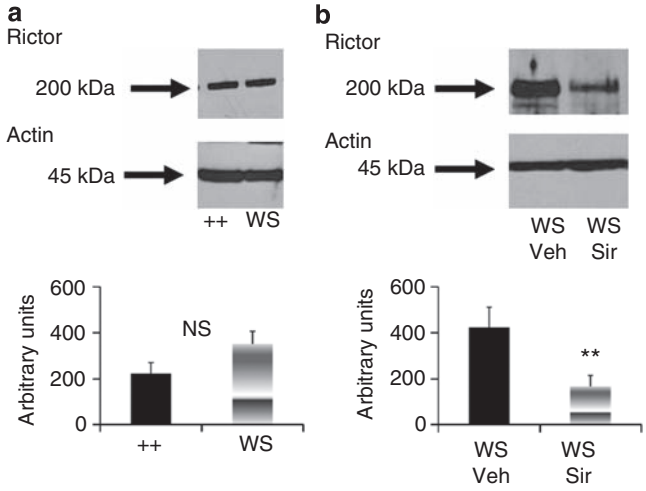

Figure 6 | Rictor immunoblot. Rictor is increased in Pkd2WS25/− kidneys (WS) compared with normal littermate controls (+ +) (**a**). Rictor is decreased in Pkd2WS25/− kidneys treated with sirolimus (WS Sir) compared with Pkd2WS25/− kidneys treated with vehicle (WS Veh) (**b**). Actin used as a loading control was equal in all the groups. Densitometry for Rictor reflects six separate experiments. NS, not significant, $^{**}P<0.05$ vs WS Veh.

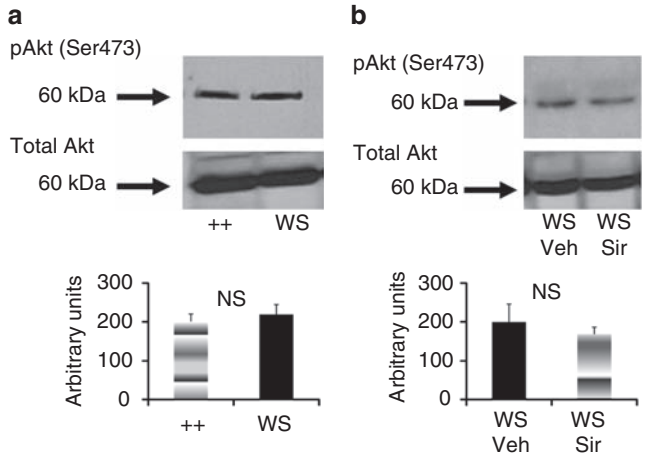

Figure 7 | Phospho-Akt (serine 473) immunoblot. Phospho-Akt (serine 473) induces proliferation and inhibits apoptosis. Phospho-Akt (serine 473) is directly phosphorylated by the mTOR–Rictor or mTORC2 complex and is a marker of mTORC2 activity. Phospho-Akt (serine 473) was not increased in Pkd2WS25/− kidneys (WS) compared with littermate controls (+ +) (**a**). Phospho-Akt (serine 473) was not different between Pkd2WS25/− kidneys treated with vehicle (WS Veh) compared with Pkd2WS25/− kidneys treated with sirolimus (WS Sir) (**b**). Total Akt used as a control was not different between the groups. Densitometry for Phospho-Akt (serine 473) reflects six separate experiments. NS, not significant.

sirolimus had no inhibitory effect on levels of phospho-AKT (serine 473) (Figure 7b).

DISCUSSION

Two mutations have been induced in the mouse homolog *Pkd2* gene: an unstable allele (WS25; also known as Pkd2WS25/− mice) that can undergo homologous recombination-based somatic rearrangement to form a null allele; and a true null mutation (WS183; also known as Pkd2−/− mice).[16] Adult Pkd2 + /− mice have intermediate survival in the absence of cystic disease or renal failure, providing the first indication of a deleterious effect of haploinsufficiency of Pkd2 on long-term survival. As in human ADPKD, formation of kidney cysts in adult Pkd2WS25/− mice is associated with renal failure and early death. The vasopressin V2 receptor antagonist OPC31260 decreases renal CVD and BUN in Pkd2WS25/− mice.[17] Treatment of Pkd2WS25/− mice between 4 and 8 months of age with the VEGFR inhibitor, SU-5416, markedly reduced liver weight and CVD of the liver.[18] These adult Pkd2WS25/− mice were used in this study. Study of mice with targeted mutations of the PKD

gene have advanced our understanding of ADPKD as these mouse models recapitulate the complex human ADPKD phenotype.[19]

Human and experimental data provide strong evidence that abnormal proliferation in tubular epithelial cells has a crucial role in cyst development and/or growth in PKD.[20] Genetic manipulations that induce the proliferation of tubular epithelial cells in mice cause cysts to form in the kidney.[21,22] The therapeutic effect of sirolimus in PKD is related to its anti-proliferative effect. Although the proliferation index is consistently highest in cystic tubular epithelium, non-cystic tubules from mice suffering with PKD[23] and Han:SPRD rats[1,24] have higher proliferation rates than tubules from age-matched controls. These studies suggest that tubular cell proliferation precedes cyst formation in the Han:SPRD rat.[24] In Pkd2WS25/− mice, increased cell proliferation is an early event preceding cyst formation.[25] In this study non cystic tubules from Pkd2WS25/− mice had higher expression of phospho-S6 protein than non cystic tubules from wild-type mice (Figure 4) suggesting that activation of the mTORC1 signaling pathway is an early event preceding cyst formation. In this study, sirolimus therapy was started at 4–8 weeks of age, a time when there is already significant proliferation and kidney cyst formation in Pkd2WS25/− mice.[16,25] Thus, it is likely that initiation of therapy earlier would have had a better therapeutic effect. On the other hand sirolimus therapy initiated after significant proliferation and cyst formation, as in this study, still had a therapeutic effect. Thus, this study has implications for the treatment of patients, which in many cases will be initiated after significant cyst formation.

The Pkd2WS25/− mice had a 2K/TBW ratio that was nearly double that of normal littermate control mice. The Pkd2WS25/− mice had chronic kidney disease as indicated by a BUN concentration that was double that of normal littermate control mice. Sirolimus significantly decreased kidney and cyst size but had no effect on the chronic kidney disease as assessed by the BUN. Although an inverse relationship between increasing cyst volume and decreasing kidney function is known,[26] it is shown that the 51% decrease in CVD caused by sirolimus was not enough to affect renal function in Pkd2WS25/− mice.

Therapeutic blood levels of sirolimus in humans are 5–15 ng/ml. The mean trough sirolimus levels in '+ +' and 'ws25' mice was above therapeutic levels. The high blood levels raise the possibility that sirolimus nephrotoxicity may have contributed to the lack of an effect of sirolimus on BUN. However, sirolimus has minimal functional and histopathological effects in normal rat and mouse kidney. In Sprague–Dawley rats, sirolimus (10 mg/kg/d), a dose three times higher than its effective immunosuppressive dose, had no functional or histological effects on the kidney.[27] In mice, sirolimus (up to 100 mg/kg), a dose 50 times higher than its therapeutic dose, reduced body weight after 7 days but had minimal effect on kidney function and histology.[28] Thus, as opposed to cyclosporin, we do not think that there was nephrotoxicity due to sirolimus. In addition, unlike Han:SPRD rats treated with sirolimus (0.2 mg/kg/d) for 5 weeks[1] or 1 year[29] that 22% loss in body weight, the Pkd2WS25/− mice or normal littermate control mice treated with 0.5 mg/kg/d did not experience weight loss suggesting that weight loss was not a side effect of sirolimus therapy in mice.

Next we sought to determine why sirolimus did not have a better therapeutic effect. It is possible that a higher dose of sirolimus or earlier initiation of therapy may have had a better therapeutic effect. As kidney size and CVD were not normalized by sirolimus, we investigated the mTORC2 pathway that is known to be proliferative through phosphorylation of phospho-Akt (serine 473).[7,13] Rictor and phospho-Akt (serine 473), the functional readout of the mTOR–Rictor mTORC2 complex activity, were not different between normal littermate control and Pkd2WS25/− kidneys at 16 weeks of age. However, Rictor in whole kidney lysates was decreased by sirolimus in Pkd2WS25/− mice. A possible reason for the difference between Rictor and phospho-Akt (serine 473) expression is that Rictor expression in whole kidney lysates does not accurately reflect mTORC2 assembly or the effect of sirolimus on mTORC2 assembly.[14,15] Rather, the Rictor-mTOR complex on immunopreciptates of cells, not whole cell lysates, reflects mTORC2 assembly and Akt (serine 473) activity.[14,15] Long term or high-dose sirolimus therapy[14,30] is able to inhibit mTORC2 assembly, as seen on immunoprecipitation, and resultant phosphorylation of Akt (serine 473).

In this study, we show activation of mTORC1 (increased ribosomal S6 protein), but not mTORC2, in PKD caused by a mutation of the *Pkd2* gene. Having shown that there is increased mTORC1 signaling in Pkd2WS25/− kidneys and that sirolimus significantly decreases kidney size and CVD in Pkd2WS25/− mice, we speculated on how the mutation in the *Pkd2* gene as seen in Pkd2WS25/− mice, may affect mTORC1 signaling. PC-2, the protein product of the *Pkd2* gene binds to polycystin-1 (PC-1), a large transmembrane receptor.[31] PC-1 and PC-2 are proposed to constitute a flow-sensitive ion channel complex in the primary cilium. It has recently been discovered that the PC-1/PC-2 ratio regulates pressure sensing.[32] The PC-1 and PC-2 proteins associate in a complex to prevent cyst formation.[7] For example, PC-1 induces the formation of a complex with tuberin and the ser/thr kinase of mTOR resulting in inhibition of mTORC1 activity.[5] Most recently, direct evidence that PC-1 inhibits mTORC1 in a tuberin-dependent manner by regulation of ERK-dependent phosphorylation was shown.[33] Thus, the PC-1/TSC-1-TSC-2 complex inhibits mTORC1.[34] In contrast, the TSC-1—TSC-2 complex activates mTORC2 in a manner that is independent of the effect of the TSC-1–TSC-2 complex on mTORC1.[34] Thus, if a mutation of PC-2 in the PC-2–PC-1 complex was acting through TSC-1/TSC-2, there would be an increase in mTORC1 and inhibition of mTORC2 in Pkd2WS25/− mice. The fact that mTORC2 was not increased in Pkd2WS25/− mice may be because of the inhibitory effect

of a mutation in the PC-2–PC-1 complex acting through TSC-1/TSC-2 to inhibit mTORC2.

A recent study by Weimbs *et al.*[35] shows that sirolimus ameliorates PKD in mice with a conditional inactivation of the *Pkd1* gene. This study shows a similar effect of sirolimus in mice with a mutation in the *Pkd2* gene. However, there are important differences between this study and the study of Weimbs *et al.* In this study, the sirolimus dose was 0.5 mg/kg intraperitoneal compared with 5 mg/kg intraperitoneal in the Weimbs study. In view of the sirolimus trough levels of 20–22 ng/ml with 0.5 mg/kg, it is unlikely that a higher dose of sirolimus would have had a better effect on the PKD. Despite a decrease in fibrosis because of sirolimus in both studies, in the Weimbs study, sirolimus normalized the BUN in PKD mice whereas in this study sirolimus had no effect on BUN. In the Weimbs study there was a marked increase in Akt (serine 473) that was decreased by sirolimus, whereas in this study there was no increase in Akt (serine 473). In the Weimbs study, sirolimus increased apoptosis of cyst lining epithelial cells whereas in this study sirolimus had no significant effect on apoptosis and caspase-3 activity. The lack of effect of sirolimus on apoptosis may be related to the data that sirolimus had no effect on mTORC2, which is known to modulate apoptosis.

In summary, we show for the first time, increased mTORC1 signaling and a therapeutic effect of sirolimus in a model of PKD due to a mutation in the *Pkd2* gene. In addition we show that phospho-Akt (serine 473), a marker of mTORC2 activation, is not different in the kidney in Pkd2WS25/− and wild-type control mice at 16 weeks of age. The relevance of these studies to clinical ADPKD is substantial and the results should provide leads to planning clinical studies in PKD. This is particularly true because of the current availability of mTOR antagonists for example, sirolimus and its analogs and their proven *in vivo* beneficial effect as immunosuppressive drugs and cancer treatments. In addition, the use of agents that inhibit both mTORC1 and mTORC2 may be an attractive future therapy.

MATERIALS AND METHODS

Animals

The study was conducted in Pkd2WS25/− mice and normal littermate control (+/+) mice. The Pkd2WS25/− mouse develops clinically detectable PKD by 12 weeks of age as evidenced by a CVD of more than 50% of the kidney and renal failure compared with +/+ control mice.[16,17,36] A colony of Pkd2WS25/− mice was established in our animal care facility from a litter that was obtained from Stefan Somlo at Yale University. The study protocol was approved by the University of Colorado Denver Animal Care and Use Committee. Mice had free access to tap water and standard rat chow.

Genotyping

C57BL/6 Pkd2 +/− and C57BL/6 Pkd2WS25/+ mice were used as breeding pairs to generate Pkd2WS25/− mice for the study. Mice were genotyped by Southern blotting.[16,18] Briefly, DNA was isolated from tail snips (Gentra Systems, Minneapolis, MN, USA) and digested overnight with *Pst*I restriction enzyme (Promega, Madison, WI, USA). The cut DNA was run on a 0.7% agarose gel and transferred onto nylon membranes overnight. A DNA probe specific to the recombinant region was labeled with 32P by random priming (Decaprime II, Ambion, Austin, TX, USA). The probes were incubated with the blots overnight. Labeled blots were washed and developed by autoradiography. The kdS25/− mice closely model the human condition by having one copy of *Pkd2* knocked out and having a second, recombinant-sensitive allele (that is, *WS25*) that undergoes high rates of recombination to yield knockouts of the second copy of the gene in somatic cells during the lifespan of the animals.

Experimental protocol

Litters from Pkd2 +/− mice crossed with Pkd2WS25/+ mice were weaned at 3 weeks of age and then genotyped—a process that can take up to 2 weeks. Sirolimus was obtained from LC Laboratories, Woburn, MA, USA and a 1 mg/ml stock solution in 100% ethanol was kept at −20°C. Mice were treated with sirolimus 0.5 mg/kg/d intraperitoneally or vehicle (10% ethanol in normal saline) from 4–16 weeks of age. This interval of treatment and the use of both male and female mice is selected on the basis of previous studies.[16,17] In four Pkd2WS25/− mice in the vehicle control group and four Pkd2WS25/− mice in the sirolimus group, treatment was started at 6–8 weeks of age because of a delay in genotyping. Despite the delay in initiation of treatment all four mice had a decrease in 2K/TBW (%) and CVD compared with controls. Animals that were genotyped after 8 weeks of age were excluded from the study. This dose and route of administration of sirolimus is effective in C57BL6 mice with heart allograft rejection,[37] cardiac hypertrophy,[38] and regenerating liver.[39]

At the end of the 16th week of age, mice were anesthetized by intraperitoneal injection of pentobarbital sodium (50 mg/kg body weight) and kidneys were removed and weighed. The left kidney was fixed in 4% paraformaldehyde in phosphate-buffered saline for 120 min and then put into 70% ethanol and embedded in paraffin for histological examinations. The right kidney was frozen in liquid nitrogen and then stored at −80°C.

Sirolimus levels

Sirolimus was administered daily intraperitoneally. Sirolimus levels were measured using liquid chromatography/mass spectrometry by the Clinical Laboratory at University Hospital. Trough levels of sirolimus were measured just before the next dose at 16 weeks of age. Mean levels of sirolimus (ng/ml) were 22 ± 1 in +/+ mice ($n = 3$) and 20 ± 2 in Pkd2WS25/− mice ($n = 5$).

CVD

Hematoxylin-eosin stained sections were used to determine the CVD. This was carried out by a reviewer, blinded to the identity of the treatment modality, using point-counting stereology.[40] In Pkd2WS25/− mice, 80% of the cysts originate from distal nephron segments.[16] At least ten areas of the medulla at 90 degrees, 180 degrees, and 270 degrees from the hilum of each section were selected to guard against field selection variation.

Immunohistochemistry

Immunohistochemical detection of phospho-S6 ribosomal protein (ser235/236) was carried out using a donkey-anti-rabbit antibody (Cell Signaling Technology, Beverly, MA, USA catalog number 2211). Slides were deparaffinized and rehydrated. Antigen unmasking was carried out with citrate buffer. Quenching was then

performed using 3% hydrogen peroxide. Blocking was performed with Tris-buffered saline and donkey serum. A donkey anti-rabbit HRP conjugated secondary antibody was used. The sections were incubated with DAB substrate kit for peroxidase (Vector Labs, Burlingame, CA, USA) and visualized with hematoxylin. Negative control sections showed no staining.

In situ detection of DNA fragmentation

The TUNEL method was used to detect *in situ* DNA strand breaks. The Deadend Colorimetirc TUNEL assay kit (Promega, Madison, WI, USA) was used. Positive and negative controls for TUNEL stain were carried out. All cells with apoptotic morphology (cellular rounding and shrinkage, pyknotic nuclei, and formation of apoptotic bodies) that stained positive with the TUNEL assay were counted.

Quantitation of tubular cell proliferation and apoptosis

The number of TUNEL positive cells per tubule was counted using a Nikon Eclipse E400 microscope (Melville, NY, USA) equipped with a digital camera connected to Spot Advanced imaging software (Version 3.5) by an observer blinded to the treatment modality, as we have previously described.[1,9] Twenty areas per sample were randomly selected at 90 degrees, 180 degrees, and 270 degrees from the hilum of each section were selected to guard against field-selection variation. To avoid confusion between non-cystic tubules and small cysts, as well as potential changes in tubular cells lining massive cysts, TUNEL-positive cells were counted in 'medium-sized cysts' of approximately 250 μm diameter.

Caspase-3 assay

The activity of caspase-3 was determined by use of flourescent substrates as we have previously described in detail.[41] Whole kidney was mixed with a lysis buffer containing 25 mM Na Hepes, 2 mM dithiothreitol, 1 mM ethylenediaminetetraacetic acid, 0.1% 3-((3-cholamidopropyl) dimethylammonio)-1-pro-panesulfonate, 10% sucrose, 1 mM phenylmethylsulfonyl fluoride and 1 μM pepstatin A, pH 7.2, and homogenized with ten strokes in a glass-Teflon homogenizer. The lysate was then centrifuged at 4°C at 100,000 × *g* in a Beckman (Fullerton, CA, USA) Ti70 rotor for 1 hr. The caspase assay was performed on the resultant supernatants (cytosolic extract). The assay buffer for caspase-3 contained 25 mM K^+ Hepes, 1 mM dithiothreitol, 0.1% 3-((3-cholamidopropyl) dimethylammonio)-1-pro-panesulfonate, 50 mM KCl, pH 7.4. Ac-Asp-Glu-Val–Asp-7-amido-4-methyl coumarin in 10% dimethyl sulfoxide was used as a susceptible substrate for caspase-3. Peptide cleavage was measured over 1 h at 30°C using a Cytofluor 4000 series fluorescent plate reader (Perseptive Biosystems, Framingham, MA, USA) at an excitation wavelength of 380 nm and an emission wavelength of 460 nm. An aminomethylcoumarin standard curve was determined for each experiment. Caspase activity was expressed in nmol aminomethylcoumarin released per minute of incubation time per mg of lysate protein.

Immunoblotting

Immunoblot analysis was carried out as we have previously described.[42] Whole kidney tissue was homogenized in lysis buffer (in mM: 5 Na_2HPO_4, 5 NaH_2PO_4, 150 NaCl, 1 ethylenediaaminetetraacetic acid, 0.1% Triton X-100, 50 NaF, 0.2 Na_3VO_4, and 0.1% β-mercaptoethanol, pH 7.2) plus proteinase inhibitors: 1 mM 4-(2-aminoethyl)benzenesulfonyl fluoride, 15 μM pepstatin A, 14 μM L-trans-epoxysuccinyl- leucylamide- (4-guanido)- butane (E-64), 40 μM bestatin, 22 μM leupeptin, and 0.8 μM aprotonin. The homogenates were centrifuged (14,000 r.p.m at 4°C for 10 min) to remove unbroken cells and debris. Supernatants were mixed with sample buffer containing 50 mM Tris-base (pH 6.8), 0.5% glycerol, 0.01% bromphenol blue, and 0.75% sodium dodecyl sulfate and heated at 95°C for 5 min. Equal amounts of protein (60 μg/lane) were fractionated by Tris-glycine-SDS–PAGE. The electrophoretically separated proteins were then transferred to a nitrocellulose membrane (Millipore, Bedford, MA, USA) by wet electroblotting. The membranes were blocked with 5% nonfat dry milk in Tris-buffered saline tween-20 (50 mM Tris (pH 7.5), 150 mM NaCl, and 0.1% Tween buffer at pH 7.5, overnight at 4°C.

Immunoblot analyses were carried out with the following antibodies: (1) A phosho-S6 ribosomal protein (ser235/236) antibody (Cell Signaling Technology, Beverly, MA, USA, catalog number 2211) that detects ribosomal S6 protein only when phosphorylated at serine 235 and 236. The main *in vivo* S6 ribosomal protein phosphorylation sites for p70S6Kinase are ser235/236 and ser240/244.[43,44] Phospho-S6 ribosomal protein is recognized as a 32 kDa protein. (2) A S6 ribosomal protein (5G10) antibody (Cell Signaling Technology, catalog number 2217) that detects levels of total S6 protein independent of phosphorylation. Total S6 ribosomal protein is recognized as a 32 kDa protein. (3) A goat polyclonal antibody against Rictor (Santa Cruz biotechnology, Santa Cruz, CA, USA, catalog number sc-50678) that recognizes a 200 kDa protein. (4) A rabbit monoclonal antibody that detects endogenous levels of Akt only when phosphorylated at serine 473 (Cell Signaling Technology, catalog number 9271). Phospho-Akt (serine 4730) is recognized as a 60 kDa protein. (5) A rabbit monoclonal antibody that detects endogenous levels of total Akt1, Akt2 and Akt 3 proteins (Cell Signaling Technology, catalog number 9272). Total Akt is recognized as a 60 kDa protein. (6) A rabbit monoclonal antibody to β-actin that recognizes a 45 kDa protein (Cell Signaling Technology, catalog number 4970).

The membranes were incubated with primary antibodies for 1 h at room temperature, washed in Tris-buffered saline tween-20 buffer, and further incubated with donkey anti-rabbit IgG or donkey anti-goat IgG coupled to horseradish peroxidase (Amersham, Piscataway, NJ, USA) at 1:1000 dilution in Tris-buffered saline tween-20 buffer for 1 h at room temperature. Subsequent detection was carried out by enhanced chemiluminescence (Amersham), according to the manufacturer's instructions. Prestained protein markers (BioRad, Hercules, CA, USA) were used for molecular mass determination. Chemiluminescence was recorded with a film, and results were analyzed with the 1D Image Software (Kodak Digital Science, Rochester, NY, USA). Images for densitometry were analyzed using 1D Image Software (Kodak digital Science).

Chemistry

BUN was measured using quantitative colorimetric urea determination (QuantiChrom urea assay kit-DIUR-500) (Bioassay Systems, Hayward, CA, USA).

Statistical analysis

Non-normally distributed data were analyzed by the nonparametric unpaired Mann–Whitney test. Multiple group comparisons were carried out using two-way analysis of variance (GraphPad Prism Version 4). A *P*-value of <0.05 was considered statistically significant. Values are expressed as means ± s.e.

DISCLOSURE

All the authors declared no competing interests.

ACKNOWLEDGMENTS

This study was supported by NIH DK074835 (CLE), NIH DK07483503S1 (CLE), NIH Minority Supplement (FAB), PKD Foundation Bridging Grant (CLE), and Wyeth Investigator-initiated grant (RBD).

REFERENCES

1. Tao Y, Kim J, Schrier RW *et al.* Rapamycin markedly slows disease progression in a rat model of polycystic kidney disease (PKD). *J Am Soc Nephrol* 2005; **16**: 46–51.
2. Wahl PR, Serra AL, Le Hir M *et al.* Inhibition of mTOR with sirolimus slows disease progression in Han:SPRD rats with autosomal dominant polycystic kidney disease (ADPKD). *Nephrol Dial Transplant* 2006; **21**: 598–604.
3. Wu M, Wahl PR, Le Hir M *et al.* Everolimus retards cyst growth and preserves kidney function in a rodent model for polycystic kidney disease. *Kidney Blood Press Res* 2007; **30**: 253–259.
4. Shillingford JM, Murcia NS, Larson CH *et al.* The mTOR pathway is regulated by polycystin-1, and its inhibition reverses renal cystogenesis in polycystic kidney disease. *Proc Natl Acad Sci USA* 2006; **103**: 5466–5471.
5. Weimbs T. Regulation of mTOR by polycystin-1: is polycystic kidney disease a case of futile repair? *Cell Cycle* 2006; **5**: 2425–2429.
6. Fischer DC, Jacoby U, Pape L *et al.* Activation of the AKT/mTOR pathway in autosomal recessive polycystic kidney disease (ARPKD). *Nephrol Dial Transplant* 2009; **24**: 1819–1827.
7. Boletta A. Emerging evidence of a link between the polycystins and the mTOR pathways. *Pathogenetics* 2009; **2**: 6.
8. Edelstein CL. What is the role of tubular epithelial cell apoptosis in polycystic kidney disease (PKD)? *Cell Cycle* 2005; **4**: e141–e145.
9. Tao Y, Kim J, Faubel S *et al.* Caspase inhibition reduces tubular apoptosis and proliferation and slows disease progression in polycystic kidney disease (PKD). *Proc Natl Acad Sci USA* 2005; **102**: 6954–6959.
10. Witzgall R. Polycystic kidney disease–a tale of calcium channels and the actin cytoskeleton. *Anna Anat* 2001; **183**: 391–392.
11. Boca M, D'Amato L, Distefano G *et al.* Polycystin-1 induces cell migration by regulating phosphatidylinositol 3-kinase-dependent cytoskeletal rearrangements and GSK3beta-dependent cell cell mechanical adhesion. *Mol Biol Cell* 2007; **18**: 4050–4061.
12. Doctor RB, Serkova N, Hasebroock K *et al.* Distinct patterns of kidney and liver cyst growth in Pkd2WS25/− mice. *Nephrol Dial Transplant* 2010 (in press).
13. Wullschleger S, Loewith R, Hall MN. TOR signaling in growth and metabolism. *Cell* 2006; **124**: 471–484.
14. Sarbassov DD, Ali SM, Sengupta S *et al.* Prolonged rapamycin treatment inhibits mTORC2 assembly and Akt/PKB. *Molecular Cell* 2006; **22**: 159–168.
15. Toschi A, Lee E, Xu L *et al.* Regulation of mTORC1 and mTORC2 complex assembly by phosphatidic acid: competition with rapamycin. *MolCell Biol* 2009; **29**: 1411–1420.
16. Wu G, Markowitz GS, Li L *et al.* Cardiac defects and renal failure in mice with targeted mutations in Pkd2. *Nat Genet* 2000; **24**: 75–78.
17. Torres VE, Wang X, Qian Q *et al.* Effective treatment of an orthologous model of autosomal dominant polycystic kidney disease. *Nat Med* 2004; **10**: 363–364.
18. Amura CR, Brodsky KS, Groff R *et al.* VEGF receptor inhibition blocks liver cyst growth in pkd2(WS25/−) mice. *Am J Physiol Cell Physiol* 2007; **293**: C419–C428.
19. Somlo S, Markowitz GS. The pathogenesis of autosomal dominant polycystic kidney disease: an update. *Curr Opin Nephrol Hypertens* 2000; **9**: 385–394.
20. Wilson PD. Polycystic kidney disease. *N Engl J Med* 2004; **350**: 151–164.
21. Trudel M, D'Agati V, Costantini F. C-myc as an inducer of polycystic kidney disease in transgenic mice. *Kidney Int* 1991; **39**: 665–671.
22. Schaffner DL, Barrios R, Massey C *et al.* Targeting of the rasT24 oncogene to the proximal convoluted tubules in transgenic mice results in hyperplasia and polycystic kidneys. *Am J Pathol* 1993; **142**: 1051–1060.
23. Trudel M, Barisoni L, Lanoix J *et al.* Polycystic kidney disease in SBM transgenic mice: role of c-myc in disease induction and progression. *Am J Pathol* 1998; **152**: 219–229.
24. Ramasubbu K, Gretz N, Bachmann S. Increased epithelial cell proliferation and abnormal extracellular matrix in rat polycystic kidney disease. *J Am Soc Nephrol* 1998; **9**: 937–945.
25. Chang MY, Parker E, Ibrahim S *et al.* Haploinsufficiency of Pkd2 is associated with increased tubular cell proliferation and interstitial fibrosis in two murine Pkd2 models. *Nephrol Dial Transplant* 2006; **21**: 2078–2084.
26. Chapman AB, Guay-Woodford LM, Grantham JJ *et al.* Glockner JF, Wetzel LH, Brummer ME, O'Neill WC, Robbin ML, Bennett WM, Klahr S, Hirschman GH, Kimmel PL, Thompson PA, Miller JP, Consortium for Radiologic Imaging Studies of Polycystic Kidney Disease, cohort: Renal structure in early autosomal-dominant polycystic kidney disease (ADPKD): The Consortium for Radiologic Imaging Studies of Polycystic Kidney Disease (CRISP) cohort. *Kidney Int* 2003; **64**: 1035–1045.
27. DiJoseph JF, Sharma RN, Chang JY. The effect of rapamycin on kidney function in the Sprague-Dawley rat. *Transplantation* 1992; **53**: 507–513.
28. Di Joseph JF, Sehgal SN. Functional and histopathologic effects of rapamycin on mouse kidney. *Immunopharmacol Immunotoxicol* 1993; **15**: 45–56.
29. Zafar I, Belibi FA, He Z *et al.* Long-term rapamycin therapy in the Han:SPRD rat model of polycystic kidney disease (PKD). *Nephrol Dial Transplant* 2009; **24**: 2349–2353.
30. Zeng Z, Sarbassov dD, Samudio IJ *et al.* Rapamycin derivatives reduce mTORC2 signaling and inhibit AKT activation in AML. *Blood* 2007; **109**: 3509–3512.
31. Qian F, Germino FJ, Cai Y *et al.* PKD1 interacts with PKD2 through a probable coiled-coil domain. *Nat Genet* 1997; **16**: 179–183.
32. Sharif-Naeini R, Folgering JH, Bichet D *et al.* Polycystin-1 and -2 dosage regulates pressure sensing. *Cell* 2009; **139**: 587–596.
33. Distefano G, Boca M, Rowe I *et al.* Polycystin-1 regulates extracellular signal-regulated kinase-dependent phosphorylation of tuberin to control cell size through mTOR and its downstream effectors S6K and 4EBP1. *Mol Cell Biol* 2009; **29**: 2359–2371.
34. Huang J, Dibble CC, Matsuzaki M *et al.* The TSC1-TSC2 complex is required for proper activation of mTOR complex 2. *Mol Cell Biol* 2008; **28**: 4104–4115.
35. Shillingford JM, Piontek KB, Germino GG *et al.* Rapamycin ameliorates PKD resulting from conditional inactivation of Pkd1. *J Am SocNephrol* 2010; **21**: 489–497.
36. Wu G, D'Agati V, Cai Y *et al.* Somatic inactivation of Pkd2 results in polycystic kidney disease. *Cell* 1998; **93**: 177–188.
37. Koehl GE, Andrassy J, Guba M *et al.* Rapamycin protects allografts from rejection while simultaneously attacking tumors in immunosuppressed mice. *Transplantation* 2004; **77**: 1319–1326.
38. McMullen JR, Sherwood MC, Tarnavski O *et al.* Inhibition of mTOR signaling with rapamycin regresses established cardiac hypertrophy induced by pressure overload. *Circulation* 2004; **109**: 3050–3055.
39. Goggin MM, Nelsen CJ, Kimball SR *et al.* Rapamycin-sensitive induction of eukaryotic initiation factor 4F in regenerating mouse liver. *Hepatology* 2004; **40**: 537–544.
40. Cowley Jr BD, Rupp JC, Muessel MJ *et al.* Gender and the effect of gonadal hormones on the progression of inherited polycystic kidney disease in rats. *Am J Kidney Dis* 1997; **29**: 265–272.
41. Faubel SG, Ljubanovic D, Reznikov LL *et al.* Caspase-1-deficient mice are protected against cisplatin-induced apoptosis and acute tubular necrosis. *Kidney Int* 2004; **66**: 2202–2213.
42. Shi Y, Melnikov VY, Schrier RW *et al.* Downregulation of the calpain inhibitor protein calpastatin by caspases during renal ischemia-reperfusion. *Am J Physiol Renal Physiol* 2000; **279**: F509–F517.
43. Ferrari S, Bandi HR, Hofsteenge J *et al.* Mitogen-activated 70K S6 kinase. Identification of *in vitro* 40 S ribosomal S6 phosphorylation sites. 1991; **266**: 22770–22775.
44. Flotow H, Thomas G. Substrate recognition determinants of the mitogen-activated 70K S6 kinase from rat liver. *J Biolo Chem* 1992; **267**: 3074–3078.